ISSN 2472-1972

The Catalytic Subunit β of PKA Affects Energy Balance and Catecholaminergic Activity

Edra London,[1] Audrey Noguchi,[2] Danielle Springer,[2] Maria Faidas,[1] Oksana Gavrilova,[3] Graeme Eisenhofer,[4,5] and Constantine A. Stratakis[1]

[1]Section on Endocrinology and Genetics, Eunice Kennedy Shriver National Institute of Child Health and Human Development, National Institutes of Health, Bethesda, Maryland 20892; [2]Murine Phenotyping Core, National Heart, Lung, and Blood Institute, National Institutes of Health, Bethesda, Maryland 20892; [3]Mouse Metabolism Core, National Institute of Diabetes and Digestive and Kidney Diseases, National Institutes of Health, Bethesda, Maryland 20892; [4]Department of Medicine III Techniche Universität Dresden, 01307 Dresden, Germany; and [5]Institute of Clinical Chemistry and Laboratory Medicine, Techniche Universitat Dresden, 03107, Dresden, Germany

ORCiD numbers: 0000-0003-2766-749X (E. London).

The protein kinase A (PKA) signaling system mediates the effects of numerous hormones, neurotransmitters, and other molecules to regulate metabolism, cardiac function, and more. PKA defects may lead to diverse phenotypes that largely depend on the unique expression profile of the affected subunit. Deletion of the *Prkarcb* gene, which codes for PKA catalytic subunit β (Cβ), protects against diet-induced obesity (DIO), yet the mechanism for this phenotype remains unclear. We hypothesized that metabolic rate would be increased in Cβ knockout (KO) mice, which could explain DIO resistance. Male, but not female, CβKO mice had increased energy expenditure, and female but not male CβKO mice had increased subcutaneous temperature and increased locomotor activity compared with wild-type (WT) littermates. Urinary norepinephrine (NE) and normetanephrine were elevated in female CβKO mice. CβKO mice had increased heart rate (HR); blocking central NE release normalized HR to that of untreated WT mice. Basal and stimulated PKA enzymatic activities were unchanged in adipose tissue and heart and varied in different brain regions, suggesting that *Prkacb* deletion may mediate signaling changes in specific brain nuclei and may be less important in the peripheral regulation of PKA expression and activity. This is a demonstration of a distinct effect of the PKA Cβ catalytic subunit on catecholamines and sympathetic nerve signaling. The data provide an unexpected explanation for the metabolic phenotype of CβKO mice. Finally, the sexual dimorphism is consistent with mouse models of other PKA subunits and adds to the importance of these findings regarding the PKA system in human metabolism.

Copyright © 2019 Endocrine Society

This article has been published under the terms of the Creative Commons Attribution Non-Commercial, No-Derivatives License (CC BY-NC-ND; https://creativecommons.org/licenses/by-nc-nd/4.0/).

Freeform/Key Words: PKA, catecholamines, sympathetic outflow, energy balance, cardiovascular

The cAMP-dependent protein kinase A (PKA) is essential in mediating the effects of a vast number of G-protein-coupled receptor-dependent ligands, including hormones and neurotransmitters, that modulate intracellular cAMP levels. In humans and mice, the PKA holoenzyme consists of two regulatory (R) and two catalytic (C) subunits. There are four R subunits (RIα, RIβ, RIIα, and RIIβ) and at least three C subunits (Cα, Cβ, and PRKAX). PKA

Abbreviations: AT, adipose tissue; BAT, brown adipose tissue; BCA, bicinchoninic acid; BP, blood pressure; BPM, beats/minute; C, catalytic; CβKO, protein kinase A catalytic subunit β gene knockout; CD, control diet; CT, comparative threshold; DAB, 3,3′-diaminobenzidine; DIO, diet-induced obesity; EPI, epinephrine; HFD, high-fat diet; HR, heart rate; KO, knockout; LC, locus coeruleus; MN, metanephrine; NE, norepinephrine; NMN, normetanephrine; pCREB, phosphorylated cAMP-response element-binding; PFA, paraformaldehyde; PKA, protein kinase A; q, quantitative; R, regulatory; SNAP-25, synaptosomal nerve-associated protein 25; SQ, subcutaneous; TA, total activity; TEE, total energy expenditure; Ucp1, uncoupling protein 1; WAT, white adipose tissue; WT, wild type.

Received 18 January 2019
Accepted 22 March 2019
First Published Online 28 March 2019

subunit expression varies between tissues, and this variability, along with different cAMP and A-kinase anchoring protein affinities, determines cell-specific PKA responses to cAMP generated by the binding of a ligand to the corresponding G-protein-coupled receptor. Mouse models have been instrumental in understanding the diverse roles for PKA in regulating energy balance and metabolism. Studies in mice have demonstrated that deletion of regulatory subunit RIIβ [1] or RIIα [2] or catalytic subunit Cβ [3] confers resistance to diet-induced obesity (DIO) through distinct mechanisms specific to the affected PKA subunit and the cell types in which that subunit is expressed.

In mice, dysregulated PKA activity, caused by targeted deletion of *Prkar2b* (RIIβ), caused increased energy expenditure and basal lipolysis [1, 4], as well as increased insulin [5] and leptin [6] sensitivities and these traits prevented age-related metabolic dysfunction [7]. Changes in locomotor activity were sex specific [8]. Despite the high expression of *Prkar2b* in adipose tissue (AT), altered PKA signaling in hypothalamic medial spiny neurons was the primary mediator of the observed resistance to DIO. Likewise, the *Prkar2a* knockout (KO) mouse resisted DIO and glucose intolerance and had a modestly elevated metabolic rate during a high-fat diet (HFD) [2].

Deletion of *Prkacb* in mice did not have obvious effects, as those seen in mice null for the most abundant PKA catalytic subunit *Prkaca*. *Prkacb* encodes three isoforms (Cβ1, Cβ2, and Cβ3), and Cβ2 and Cβ3 are transcribed from neural-specific promoters [9, 10]. *Prkacb* is expressed at low levels peripherally and at higher levels in the nervous system [11]. Deletion of all three isoforms in mice reportedly reduced basal PKA activity in whole brain lysate [12]. *Prkacb* KO (CβKO) mice were DIO resistant and when exposed to a HFD, had reduced fat mass and superior insulin sensitivity compared with wild-type (WT) mice [3]. There is sexual dimorphism with respect to the severity of phenotype and the specific phenotypic manifestations caused by perturbations in the PKA signaling pathway [13]. The underlying mechanism for the observed sexual dimorphism in PKA mouse models, such as potential interactions with sex hormones or regulation by the X chromosome, remains unknown.

In the face of the global obesity epidemic, there is interest in how PKA activation downstream of adrenergic receptors in AT might enhance metabolic rate and increase fat-burning capacity as a potential therapeutic target. The finding that BAT was present in adult humans and small mammals (*i.e.*, research animals) alike sparked a renewed interest in nervous-system activation of both brown AT (BAT) and brown-like AT to increase energy expenditure [14, 15]. BAT activation by a specific β3-adrenergic agonist reportedly mimicked the effect of cold-induced BAT activation on energy expenditure [16]. In mice, BAT- and white AT (WAT)-specific overexpression of *Prkaca* under the *Adipoq* promoter caused constitutive PKA activation in AT and increased energy expenditure without altered energy intake or locomotor activity [17]. This AT-specific increase in PKA activity was sufficient to prevent DIO in mice. In humans, visceral AT from patients with Cushing syndrome displayed differential regulation of PKA subunit expression that was associated with varying degrees of obesity and distribution of AT [18].

In the present investigation, we tested the hypothesis that CβKO mice have an enhanced metabolic rate as a result of PKA subunit dysregulation; the data were surprising and provided an alternate way to resistance to DIO—that of altered catecholaminergic activity. Thus, we report here a role for the Cβ PKA subunit as a central regulator of the sympathetic nervous system.

1. Materials and Methods

A. Mice and Diets

Mice null for all three *Prkacb* isoforms (CβKO), two (Cβ2 and Cβ3) of which are transcribed from neural-specific promoters, were generated, as previously described [12]. Male and female CβKO and WT mice were bred from heterozygous breeding pairs on a C57BL/6J background. Mice were maintained on a regular control diet (CD; NIH-31; Harlan-Teklad, Indianapolis, IN) and 12 hours light/dark cycle from weaning at ~21 days. For indirect

calorimetry and telemetry studies, male and female CβKO and WT littermates (11 to 12 and 17 to 22 weeks old at outset, respectively) were used. The female and male cohorts for calorimetry and telemetry each derived from two and three litters, respectively, as was the case for the RNA, protein, and PKA activity studies. Urine was collected for catecholamine quantification from the indirect calorimetry cohorts when mice were 3 months old. Tissues were collected at the end of each study, snap frozen, and stored at −80°C for subsequent expression and PKA enzymatic studies or fixed in 4% paraformaldehyde (PFA) for immunohistological analyses.

All mouse procedures were approved by and conducted in accordance with the Eunice Kennedy Shriver National Institute of Child Health and Human Development Institutional Animal Care and Use Committee.

The CD, NIH-31 Open Formula (Harlan-Teklad), had an energy density of 3.0 kcal/g with 24%, 14%, and 62% of the total energy derived from protein, fat, and carbohydrate, respectively. The HFD, used for energy balance and DIO studies, was high-fat, soft pellet chow (F3282; Bio-Serv, Frenchtown, NJ) with an energy density of 5.5 kcal/g; 21%, 36%, and 36% of energy was derived from protein, fat, and carbohydrate, respectively.

B. Indirect Calorimetry

Indirect calorimetry was performed in a 12-chamber Oxymax/Comprehensive Lab Animal Monitoring System (Columbus Instruments, Inc., Columbus, OH) on 11- to 12-week-old female and male mice (n = 5 to 6/group, one mouse/chamber, 13-minute bins). Food (CD) and water were provided *ad libitum*. Mice were acclimated to the metabolic chambers for 2 days (22°C). Respiratory exchange ratio, maximal oxygen consumption, resting and total energy expenditure (TEE), resting and total energy intake, and locomotor activity were calculated for 24 hours at 22°C. Total activity (TA) was determined by infrared beam interruption using an Opto-Varimex Mini (Columbus Instruments, Inc.). Metabolic response to the specific β3-adrenergic agonist CL316243 was assessed by administration of a 0.1mg/kg IP dose after mice were acclimated to thermoneutral conditions (29°C) for 24 hours.

C. Telemetric Measurement of Heart Rate, Blood Pressure, and Temperature, With and Without Adrenergic Agonist/Antagonist Treatment

HD-X10 blood pressure (BP) transmitters (Data Sciences International, St. Paul, MN) were subcutaneously implanted in anesthetized female and male WT and CβKO littermate mice weighing at least 20 g. A midline incision was made in the ventral surface of the neck, extending from the mandible to the level of the sternum. With the use of blunt dissection, the skin was separated from the underlying muscle, creating a subcutaneous (SQ) pouch and tunnel that began at the cervical incision and extended to the lateral chest and flank. Transmitters were placed in the SQ pouch. The glands in the neck were retracted to expose the muscles along the trachea and the carotid artery; the latter was dissected and isolated from the vagus nerve. Two proximal suture ties were used to secure a catheter in the vessel and the distal one, near the bifurcation of the internal and external carotid arteries, to ligate the artery. A 27-gauge needle was used to puncture the vessel between the two ties to create an arteriotomy for placement of the catheter. Transmitter catheters (PA-C10) were placed into the vessel and advanced until the catheter tip was in the aortic arch. The mice were closely monitored following surgery and allowed 2 weeks to recover fully before the outset of data collection. Mice were individually housed and maintained on a 12-hour light/dark cycle at 23°C. Basal telemetric data for separate cohorts were collected during three separate 24-hour periods to ensure reproducibility.

D. Drugs Used for Telemetric Adrenergic Receptor Agonist and Antagonist Studies

The cardiovascular impact of adrenergic receptor stimulation and blockade was evaluated by administration (IP) of β- and α-adrenergic receptor agonists, with or without their respective antagonists, in telemetered mice. Pharmaceutical (United States Pharmacopeia)-grade

Isoproterenol Hydrochloride powder (Spectrum, Irvine, CA), prepared in sterile 0.9% saline, was administered (IP) at a dose of 50 mg/kg, as slightly modified from a previously described dose [19]. Injectable Duraclon (clonidine) was administered at a dose of 40 μg/kg [19]. Injectable propranolol and phentolamine mesylate were administered at a dose of 5 mg/kg, as previously published [20, 21]. All drugs were procured through the Department of Veterinary Research Pharmacy, National Institutes of Health (Bethesda, MD).

E. Weight Gain and Body Composition

Mice were weighed at baseline and then weekly at 0900 hour during the experimental period and at time of euthanasia for feeding and growth-curve studies. Body composition was measured at the conclusion of the 10-week CD/HFD feeding study by the EchoMRI 100H body composition analyzer for mice (EchoMRI, Houston, TX). For long-term body composition and growth studies, body composition was measured at 3, 6, and 9 months in CD-fed WT and CβKO derived.

F. Tissue and Serum Collection

Mice were euthanized by slow replacement of air with CO_2, followed by cervical dislocation. Dissected tissues were snap frozen in liquid nitrogen and stored (−80°C). Hypothalami and locus coeruleus (LC) were dissected from whole brains for a PKA enzymatic activity assay. Hypothalami were cut from the ventral side of the whole brain in a block to include both anterior and posterior portions. For LC dissection, ~200 μM-thick coronal sections were cut from the hindbrain (Bregma: ~−5.4 to 5.6 mm). LC was identified under a dissecting microscope (Nikon, Tokyo, Japan) by locating the distal and lateral edges of the fourth ventricle and tracing straight downward along the interior edges of the mesencephalic trigeminal tract. Preliminary staining for tyrosine hydroxylase of 20 μM coronal sections from the same region of the hindbrain was used to confirm the location and landmarks used. For immunohistochemistry, dissected tissues were rinsed in PBS and immediately placed into ice-cold 4% PFA and postfixed for 24 hours; brains were dissected from mice perfused with PBS and 4% PFA. Blood was collected by cardiac puncture into serum separator tubes before storage at −20°C (Becton, Dickson and Co., Franklin Lakes, NJ).

G. qRT-PCR and qRT-PCR Tissue Array Analysis

For qRT-PCR, RNA was extracted from BAT using Trizol and quantified by NanoDrop. cDNA was generated from 1 μg total RNA using the SuperScript III First Strand Synthesis System (Invitrogen, Waltham, MA). Previously tested primers were used for both qRT-PCR and the tissue array analysis (Table 1). Melt-curve analysis and gel electrophoresis were used to confirm amplification of the expected PCR product. For qRT-PCR tissue array, primers for *Prkacb* and *Gapdh* were used on two separate 96-well plates for the analysis of normal (WT) mouse tissues, according to the manufacturer's instructions (catalog no. MNRT101; OriGene,

Table 1. List of Primers Used for qRT-PCR

Target Gene	Forward Primer Sequence, 5′–3′	Reverse Primer Sequence, 5′–3′	Size, bp
Actb	CCTAGGCACCAGGGTGTG	CTTCTCCATGTCGTCCCAGT	141
Cidea	GACAGAAATGGACACCGGGT	GTATGTGCCCGCATAGACCA	269
Cox8b	AAAGCCCATGTCTCTGCCAA	GCTAAGACCCATCCTGCTGG	113
Dio2	CCTCTTCCTGGCGCTCTATG	TCAGGATTGGAGACGTGCAC	213
Pgc1a	AAAGCAATTGAAGAGCGCCG	TCGTTCGACCTGCGTAAAGT	218
Prdm16	GCCTAACTTTCCCCACTCCC	GACATCTGGGGGTGGAACAG	504
Prkacb	GGGGGAGAGATGTTCTCACA	ACCTGGATGTAACCCTGGTG	173
Ucp1	GGGCCCTTGTAAACAACAAA	GCCACAAACCCTTTGAAAAA	220

Rockville, MD). Primer sequences for *Prkacb* are provided in Table 1; *Gapdh* primers were manufacturer provided. Comparative threshold (CT) values from each plate were analyzed by use of the mean *Gapdh* CT value to then calculate the *Gapdh* factor to normalize values for the sample set using the following formula: $2^{(\text{mean } Gapdh - Gapdh \text{ CT value})}$. The *Prkacb* factor was then determined based on the lowest CT value in the sample set with the following formula: $2^{(\text{lowest } Prkacb \text{ CT} - \text{actual } Prkacb \text{ Ct value})/Gapdh \text{ factor}}$, multiplied by 1000 to get relative expression in whole integer values.

H. Western Blotting

Tissues were homogenized in ice-cold lysis buffer [20 mM Tris (pH 7.5), 0.1 mM sodium EDTA, 1 mM dithiothreitol], with 1:100 protease and phosphatase inhibitor cocktails (EMD Biosciences, La Jolla, CA) and 0.5 mM phenylmethylsulfonyl fluoride, using a Bullet Blender and RNase-free beads (Next Advance, Averill Park, NY). Total protein was quantified by bicinchoninic assay (BCA; Pierce, Rockford, IL). Membranes were generated by the loading of 20 μg total protein per well onto 4% to 12% Bis-Tris gels and transferred onto nitrocellulose membranes for 1 hour at 100 V. Before blotting, membranes were stained with Ponceau S stain and imaged to ensure uniform protein distribution across lanes. Immunoblotting was performed with the following commercially available primary antibodies: rabbit anti-PKA Cα (1:1000; catalog no. sc-903; RRID:AB_2268772 [22]; Santa Cruz Biotechnology, Dallas, TX), mouse anti-PKA RIα (1:800; catalog no. 610610; RRID:AB_397944 [23]; BD Bioscience, San Jose, CA), and goat anti-uncoupling protein 1 (Ucp1; 1:1000; catalog no. 6528; RRID:AB_2304265 [24]; Santa Cruz Biotechnology), and peroxidase-conjugated secondary antibodies: anti-goat IgG (RRID:AB_2340390 [25]), anti-rabbit IgG (RRID:AB_10015282 [26]), and anti-mouse IgG (RRID:AB_2340770 [27]; all Jackson ImmunoResearch Laboratories, West Grove, PA). Membranes were visualized using SuperSignal West Dura Extended Duration Chemiluminescent Substrate (Invitrogen) on a ChemiDoc imaging system, and densitometry analysis was performed to determine relative expression (ImageLab 4.0; Bio-Rad Laboratories, Hercules, CA).

I. Immunohistochemistry

Adrenal, BAT, spleen, and kidney were dissected from euthanized mice in the previously described studies. Tissues were rinsed in PBS and immediately postfixed in 4% PFA at 4°C for 24 hours. Sections were prepared from paraffin-embedded tissues (10 μM). For brain studies, mice were perfused with PBS and then 4% PFA, postfixed for 24 hours, and then cryopreserved with 30% sucrose solution before snap freezing and sectioning. For 3,3′-diaminobenzidine (DAB) staining, sections were probed with a primary antibody against tyrosine hydroxylase (mouse, 1:500; RRID:AB_572268 [28]; ImmunoStar, Hudson, WI) and then with peroxidase-conjugated anti-mouse IgG secondary antibody (ImPRESS; RRID:AB_2336528 [29]; Vector Laboratories, Burlingame, CA) and developed with DAB peroxidase substrate for 30 seconds (ImPACT DAB; Vector Laboratories). Sections were counterstained with hematoxylin before mounting. For immunofluorescence, BAT sections were first probed with rabbit anti-phosphorylated cAMP-response element-binding (pCREB; s133; 1:400; RRID:AB_2561044 [30]; Cell Signaling Technology, Danvers, MA) or goat anti-Ucp1 (1:400; RRID:AB_2304265 [24]; Santa Cruz Biotechnology) and then with Alexa Fluor 555 donkey anti-rabbit or anti-goat IgG (heavy chain + light chain) secondary antibodies (1:500; RRID:AB_162543 [31] and RRID:AB_2535853 [32], respectively; Invitrogen). Brain sections were probed with rabbit anti-PKA Cβ (1:400; RRID:AB_2783820 [33]; kindly provided by G. Stan McKnight, University of Washington, Seattle, WA), specific to PKA catalytic subunit β, unlike commercially available antibodies that detect both PKA Cα and Cβ; sections were then probed with donkey anti-rabbit IgG Alexa Fluor 647 secondary antibody (1:400; RRID:AB_2536183 [34]; Invitrogen). Sections were counterstained with A 4′,6-diamidino-2-phenylindole nuclear stain (1:1000; Thermo Fisher Scientific, Waltham, MA). Microphotographs were taken using uniform exposure settings between groups that were determined for each tissue type across samples (KEYENCE America, Itaska, IL).

J. PKA Activity

Hypothalamus, LC, heart, adrenal gland, BAT, and SQ WAT samples were homogenized with a Bullet Blender tissue homogenizer and appropriate grade lysis beads (Next Advance) in ice-cold buffer [10 mM Tris-HCl (pH 7.5), 1 mM EDTA, 1 mM dithiothreitol], with protease inhibitor cocktail I and phosphatase inhibitors (EMD Biosciences) and 0.5 mM phenylmethylsulfonyl fluoride. Hypothalami were dissected from whole brain under a dissecting microscope (SMZ 1500; Nikon). Cell lysates were centrifuged for 10 minutes at 4°C (10,000 *g*). Total protein concentrations were determined by BCA or micro-BCA assay (adrenal glands, hypothalami, LC; Pierce). PKA enzymatic activity was measured using a previously described method that uses ^{32}P-labeled ATP and Kemptide substrate, with or without added cAMP (5 μM) [35]. Calculated PKA/kinase activities were normalized to total protein concentration. Specificity of assay was confirmed by duplicate reactions in the presence of a PKA inhibitor (5 μM).

K. Urinary Catecholamine Quantification

Urine samples were collected from 13- to 16-week-old male and female mice between 0900 and 1100 hour by picking up each mouse and directly collecting urine into a 1.5-mL microcentrifuge tube. Catecholamines and metanephrines (MNs) were quantified by liquid chromatography with tandem mass spectrometry, as previously described [36]. Urinary creatinine was quantified using a modified kinetic Jaffe reaction with a creatinine flex reagent cartridge on a Dimension EXL with LM Integrated Chemistry System (Siemens, Malvern, PA). Urine osmolality was measured with an Advanced 2020 Osmometer (Advanced Instruments Inc., Norwood, MA). Because urine creatinine values differed significantly between mutant and WT males, catecholamine levels were normalized to osmolality.

L. Tissue Norepinephrine and Epinephrine Levels

Frozen tissue (20 mg; left ventricles, salivary glands, spleen, or whole adrenal gland; n = 6 to 8/group) was homogenized in lysis buffer (0.01 N HCl, 0.15 nM EDTA, 4 mM metabisulfite) and centrifuged for 15 minutes at 4°C (13,000 *g*). Norepinephrine (NE) and epinephrine (EPI) concentrations were quantified from the resulting supernatants by high-sensitivity ELISA, following the manufacturer's protocol (DLD Diagnostika GmbH; Hamburg, Germany).

M. Statistical Analysis

Data were described using simple descriptive statistics, which were reported as means ± SEM; relative changes were described as the percent of each respective comparison. All data distributions were assessed for approximate normality with the Shapiro-Wilk test. Continuous data (mRNA and protein expression, body composition, *etc.*) were compared between two independent groups using unpaired Student's *t* tests. For body weight data, repeated-measures two-way ANOVA and Tukey's *post hoc* multiple comparisons test were used to compare differences within and between groups over time. Multiple *t* tests were used to evaluate individual differences between groups at the different time points. A *P* value of <0.05 was considered statistically significant. Data were analyzed and graphed with GraphPad Prism 7 (GraphPad Software, La Jolla, CA).

2. Results

A. Prkacb *Mutants Had Sex-Dependent Differences in Body Composition and Weight Gain*

Under normal (CD) feeding conditions, male CβKO mice had increased fat mass and decreased fat-free mass compared with WT littermates, whereas body composition did not differ among female CβKO and WT mice (Fig. 1A). Growth curves for CβKO and WT mice revealed

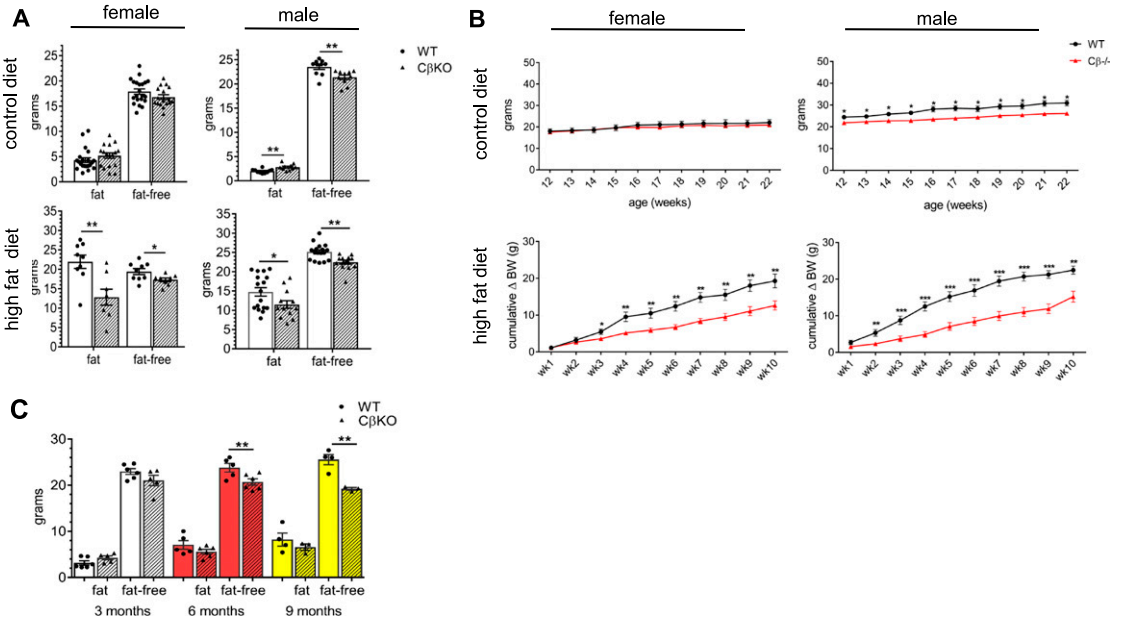

Figure 1. *Prkacb* mutants had altered weight gain and body composition as a result of chronic HFD and CD feeding that was sex dependent. (A) Fat mass and fat-free mass of female and male CβKO mice were measured by Echo-MRI after chronic feeding with either CD or HFD (n = 6 to 21/group). (B) Growth curves of female and male WT and CβKO mice during 10-wk CD or HFD feeding (n = 8 to 14/group/sex); body weight data for the HFD feeding study are shown as cumulative change in body weight from baseline. (C) Body composition of male WT and CβKO littermates at 3, 6, and 9 mo of age (n = 6 to 8/group); all data represent means ± SEM. *$P < 0.05$; **$P < 0.01$; ***$P < 0.001$. For statistical analysis, (A) two-tailed paired Student *t* tests and (B and C) repeated-measures two-way ANOVA with Tukey *post hoc* test and multiple paired *t* tests were performed.

no differences among females on a low-fat CD, but male CβKO had consistently lower body weight than WT mice chronically fed a CD (Fig. 1B; $P = 0.005$). When challenged with chronic HFD feeding for 10 weeks, both female and male CβKO mice gained less weight than their same-sex littermate controls (Fig. 1B; $P = 0.005$, $P < 0.0001$). Differences in weight gain during HFD feeding became significant between groups at weeks 2 and 3, respectively, for males and females (Fig. 1B). The attenuated weight gain derived from decreased fat mass and to a lesser degree, decreased fat-free mass (Fig. 1A). Decreased fat-free mass, regardless of diet, appeared to be a phenomenon unique to adult CβKO males, a phenotype that emerged in young adulthood, and was not apparent earlier in the life cycle (Fig. 1C).

B. Energy Expenditure Was Higher in Male CβKO Compared With WT Mice, and Female CβKO Mice Had Increased Locomotor Activity

Metabolic parameters, measured by indirect calorimetry, were normalized to lean body mass. TEE was increased in male CβKO compared with WT mice (Fig. 2A). Whereas food intake was not significantly different between CβKO and WT mice, female CβKO tended to consume more than WT female and WT and CβKO male mice (Fig. 2B). TA, measured by beam breaks, was significantly higher in female mutant compared with WT mice (Fig. 2C); this was confirmed in an additional cohort of female mice (data not shown). To explore differences further in locomotor activity and possible differences in motivated behavior, voluntary wheel running was studied in a separate cohort, but no differences were observed (data not shown).

We subsequently measured PKA enzymatic activity in BAT, SQ AT, and hypothalamus *in vitro* and found that neither basal nor total (cAMP-stimulated) PKA enzymatic activities

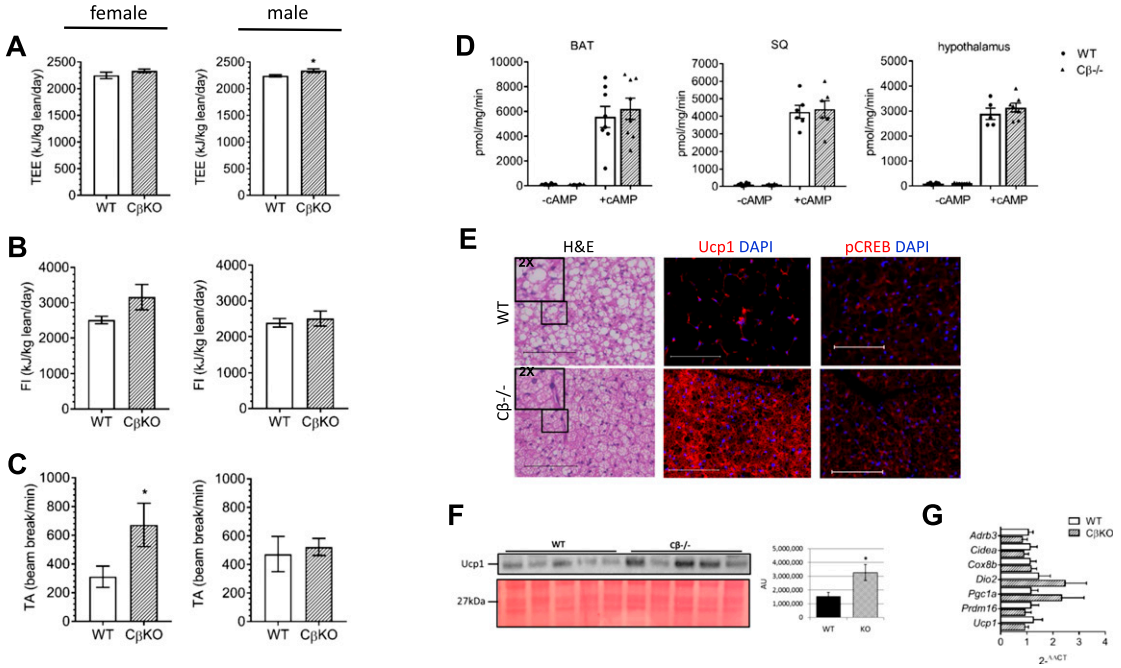

Figure 2. Metabolic rate and energy in CβKO mice compared with WT littermates. (A) TEE, (B), food intake (FI), and (C) TA during CD feeding were measured in individually housed female and male mice for 4 d at ambient (22°C) temperature; values were adjusted for lean body mass (in kilograms; n = 5 to 7/group/sex). (D) Representative PKA enzymatic activity in BAT, SQ AT (inguinal WAT), and hypothalamus, with and without cAMP stimulation (5 μM; n = 6/group, females). (E) Representative hematoxylin and eosin (H&E) and immunofluorescent staining of BAT for Ucp1 and pCREB (Ser133). Original scale bars represent 100 μM (n = 3/group, males). Inset H&E images are 2X magnified from the areas indicated. (F) Representative Western blot for Ucp1 and densitometry analysis in BAT (n = 5/group, females). (G) Relative mRNA expression of several important regulatory BAT genes was quantified by qRT-PCR. Fold change calculated as $2^{-\Delta\Delta CT}$. *Actb* was the housekeeper gene (n = 6 to 7/group, females). All values represent means ± SEM. *$P < 0.05$ compared by two-tailed Student *t* tests. AU, arbitrary unit; DAPI, 4′,6-diamidino-2-phenylindole.

differed in CβKO mutants (Fig. 2D). Whereas an *in vitro* PKA enzymatic assay cannot replicate the native microenvironment of the cells assayed, it is a good index of the compensatory regulation of PKA subunit expression.

Immunohistological analysis of BAT showed morphological differences in BAT from WT compared with CβKO mice (Fig. 2E). Hematoxylin and eosin staining of BAT revealed smaller adipocyte size and less lipid accumulation. Denser mitochondria were evident in mutant mice, as seen by the increased intensity of eosin that effectively stains mitochondria. Staining for Ucp1 was visibly much more intense, and pCREB staining also appeared to be greater in CβKO mice, which was suggestive of increased activation of BAT (Fig. 2E). The increase in Ucp1 protein in BAT of CβKO mice was confirmed by Western blot to be greater than two times higher than WT mice (Fig. 2F). Whereas mRNA levels of *Dio2* and *Pgc1a* tended to be higher in mutant BAT, none of the mRNA levels of genes examined were statistically different than those of WT mice (Fig. 2G).

C. Prkacb *Was Differentially Expressed Peripherally in Mice With the Highest Relative Expression in the Brain*

To better understand the metabolic phenotype, we evaluated mRNA expression of *Prkacb* in adult WT C57BL/6J mouse tissues. *Prkacb* was most highly expressed in brain (Fig. 3A). There was also relatively high expression of *Prkacb* in the heart, kidney, liver, epididymis, small intestine, spinal cord, and thymus (Fig. 3A). Despite the relatively high expression of

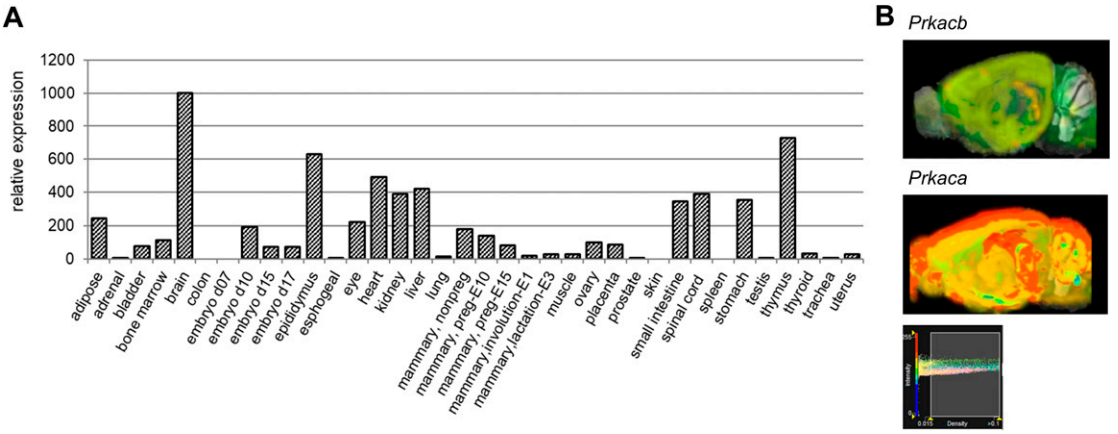

Figure 3. *Prkacb* is differentially expressed, peripherally and centrally, in mice with highest levels in the brain. (A) Relative *Prkacb* mRNA expression levels in adult WT mouse (C57BL/6) were determined by a qRT-PCR tissue array (OriGene) for normal mouse tissues and normalized to *Gapdh*. (B) Comparison of brain expression of *Prkacb* and *Prkaca* in the normal WT adult mouse brain. *In situ* expression experiments by the Allen Institute (Mouse Brain Atlas, http://mouse.brain-map.org/search/show?page_num=0&page_size=26&no_paging=false&exact_match=false&search_term=Prkacb&search_type=gene), and heat map images are shown. Full RNA *in situ* data are available at http://mouse.brain-map.org/experiment/show/532575 (image credit: Allen Institute; Fig. 3B).

Prkacb in the mouse brain, the most abundant PKA catalytic subunit (*Prkaca*) is expressed at much higher levels (Fig. 3B; adapted from images from the Allen Institute, Seattle, WA). PKA expression studies in mouse brain have demonstrated considerable specificity in the expression profiles of the PKA Cα and Cβ subunits across brain nuclei [37], which are consistent with our data.

D. CβKO Mice Had Increased Heart Rate, and Female Mutants Had Elevated SQ Body Temperature

Basal 24-hour SQ telemetric measurements showed no differences in systolic, diastolic, or mean arterial BP between CβKO and WT mice (mean BP is shown; Fig. 4A). Heart rate (HR) was increased in both female and male mutants compared with WT mice during both light and dark cycles (Fig. 4B). Female, but not male CβKO mice had elevated SQ body temperature (Fig. 4C). SQ body temperature, recorded over 24 hours, remained relatively flat for CβKO females, as the typical increase at the onset of the dark cycle was absent in mutants.

Both PKA subunits that are known to compensate for dysregulated PKA expression or activity [38–40] (RIα and Cα) were downregulated at the protein level in the mutant mice (Fig. 4D). This was not observed in the other tissues examined as part of these studies. In line with this decrease in PKA protein expression, induction of PKA by cAMP was decreased in CβKO hearts when measured *in vitro* (Fig. 4E). Basal PKA activity did not differ from that of WT mice, likely because the stoichiometry of PKA subunits was unchanged and was still permissive of normal basal PKA activity levels (data not shown). Additionally, the average heart weight of adult mutant mice was lower (Fig. 4D). Differences remained significant after corrected for body weight (data not shown).

E. Urinary NE and Normetanephrine Were Elevated in Female CβKO Mice

To determine whether altered catecholamine levels might contribute to the observed metabolic and cardiovascular phenotype, we measured urinary catecholamines. The panel of

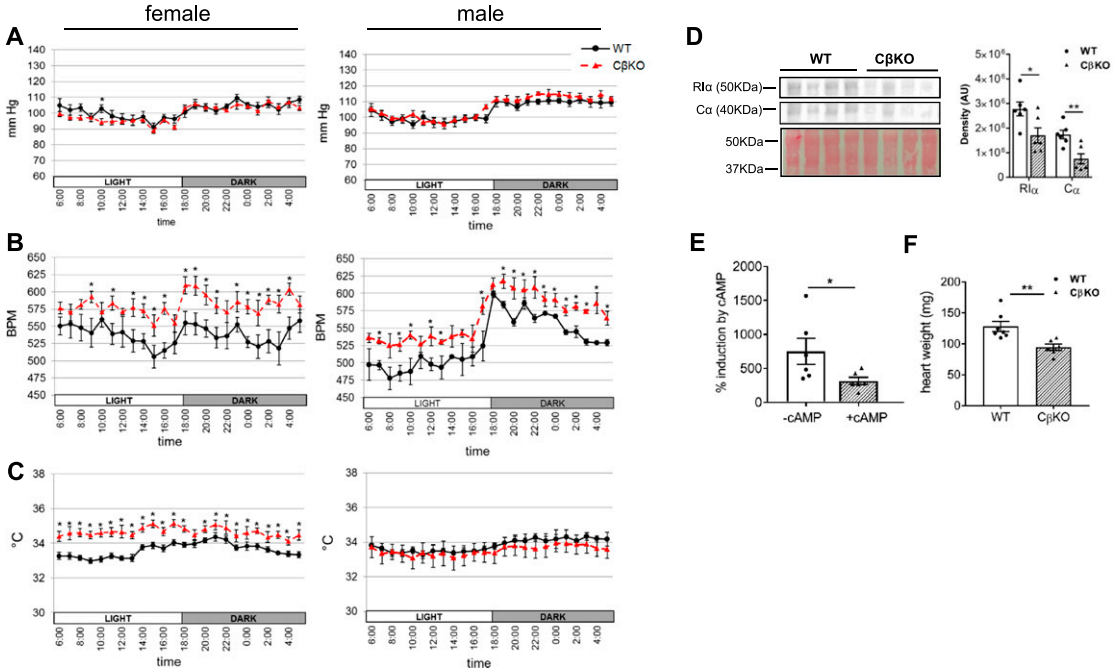

Figure 4. Heart rate (HR) was elevated in CβKO mice. Mean 24-h telemetric measurement of (A) mean arterial BP, (B) HR, and (C) SQ temperature in female and male WT and CβKO mice (n = 6/group/sex). (D) Protein expression of PKA RIα and Cα subunits in heart: representative Western blot and densitometry analysis (n = 6/group, females). (E) PKA enzymatic activity, shown as percent induction by cAMP (5 μM) in the heart (n = 6/group, females) (F) Average heart weight of female WT and CβKO littermates. Data represent means ± SEM. $*P < 0.05$; $**P < 0.01$ compared by multiple two-tailed Student t tests. BPM, beats/min.

catecholamines quantified included: normetanephrine (NMN), MN, methoxytyramine, NE, EPI, and dopamine. Urine samples were derived from age-matched WT and CβKO mice. NE and NMN were both significantly increased in female CβKO compared with WT mice (Fig. 5A), but no differences in urinary catecholamines were detected in male mice (Fig. 5B).

Urinary NE is derived largely from circulating NE and thus, reflects the small amount of NE that escapes neuronal and extraneuronal uptake to enter the bloodstream after release from sympathetic nerves [41]. NE in sympathetic nervous system target tissues, including salivary glands, ventricles, and spleen, was also increased, whereas NE levels did not differ between genotypes in adrenal glands (Fig. 5C). To confirm the nonadrenal origin of excess catecholamines, we checked EPI levels in the adrenal gland, which were unchanged in CβKO mice (Fig. 5D), and adrenal PKA activity, which was also unchanged (data not shown). We then evaluated tyrosine hydroxylase expression in kidney, spleen, and adrenal by immunohistochemistry and confirmed that there were no obvious differences (Fig. 5E). Because we suspected that increases in catecholamines were centrally mediated and had already ruled out changes in hypothalamic PKA activity as a primary cause, we examined PKA enzymatic activity in the LC (Fig. 5F). We selected LC, as it is the brain region with the greatest population of catecholaminergic presympathetic premotor neurons [42], and *Prkacb* expression in this nucleus is high, as well as unique, with respect to other PKA catalytic subunits. cAMP-stimulated PKA enzymatic activity in LC was decreased in KO mice, and although basal PKA activity tended to be lower, it was not significantly decreased. With immunofluorescent histochemistry, we confirmed high expression of PKA Cβ in the LC—the nuclei primarily responsible for secretion of NE. As expected, expression of PKA Cβ in the LC was absent in the KO mice (Fig. 5F).

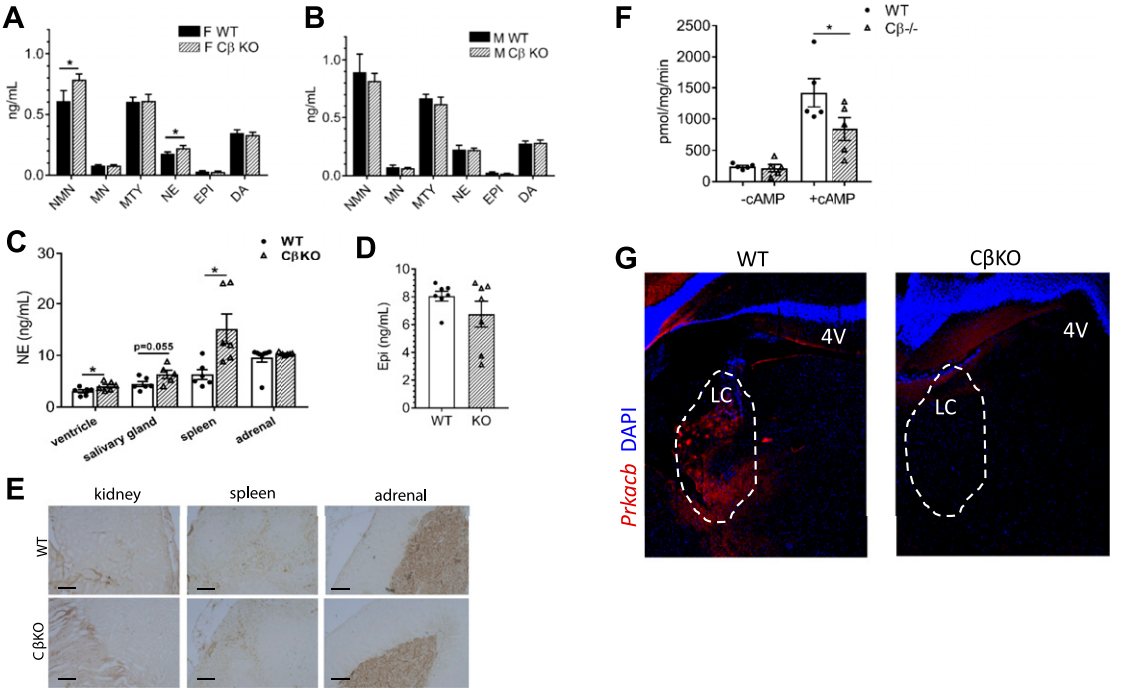

Figure 5. Urinary NE and NMN were increased in female CβKO compared with WT mice. PKA Cβ is highly expressed in LC. (A and B) Catecholamines were measured from urine collected from 3- to 4-month-old female (F) and male (M) WT and CβKO mice, generated from heterozygous breeding pairs. Catecholamines were normalized to urine osmolality (n = 6 to 10/group/sex). (C) Tissue NE concentrations in the left ventricle, salivary gland, spleen, and adrenal gland and (D) adrenal EPI levels, as quantified by high-sensitivity ELISA (female data shown). (E) Tyrosine hydroxylase immunohistochemistry in sympathetic target tissues, kidney, and spleen and in adrenal did not appear different between WT and KO mice (females). (F) Basal and total PKA enzymatic activities in LC of female mice (n = 5/group). (G) Immunofluorescent staining for PKA Cβ in coronal brain sections from female WT and mutant mice. All data are means ± SEM. *$P < 0.05$ compared by unpaired Student's t tests. 4V, fourth ventricle; DA, dopamine; MTY, methoxytyramine.

F. Pharmacologic Manipulation Revealed a Blunted Cardiovascular Response to α- and β-Adrenergic Receptor Stimulation in CβKO Mice and Blunted Metabolic Response to β3-Adrenergic Agonist in HFD-Fed Mutants; Clonidine Corrected CβKO HR to That of Untreated WT Mice

Because of the increased HR and SQ temperature (females) in conjunction with the observed increase in urinary NE and NMN, we performed telemetry studies with pharmacologic manipulation aimed at assessing the cardiovascular response to stimulation and blockade of α- and β-adrenergic receptors and to the inhibition of sympathetic outflow. We treated telemetered mice with a pan β-adrenergic receptor agonist (isoproterenol) and with clonidine, an α2-adrenergic agonist, also known to inhibit central NE release, to see if we could reverse the increased HR observed in the CβKO mice. We also tested the effects of phentolamine mesylate, an α-adrenergic antagonist, and propranolol, a β-adrenergic antagonist, on the parameters measured.

Isoproterenol decreased mean BP in both WT and CβKO mice (Fig. 6A), but the change from baseline BP (*i.e.*, magnitude of response) was greater among WT mice for a duration of 40 minutes post-treatment (Fig. 6B). Likewise, HR increased in both WT and mutant mice after isoproterenol treatment (Fig. 6C). Whereas the response to treatment tended to be blunted in mutants, the difference was not significant (Fig. 6D). It should be noted that interanimal variability in HR was considerable. After a brief, initial dip for WT mice, SQ temperature increased in response to isoproterenol in all mice (Fig. 6E), and the mean SQ

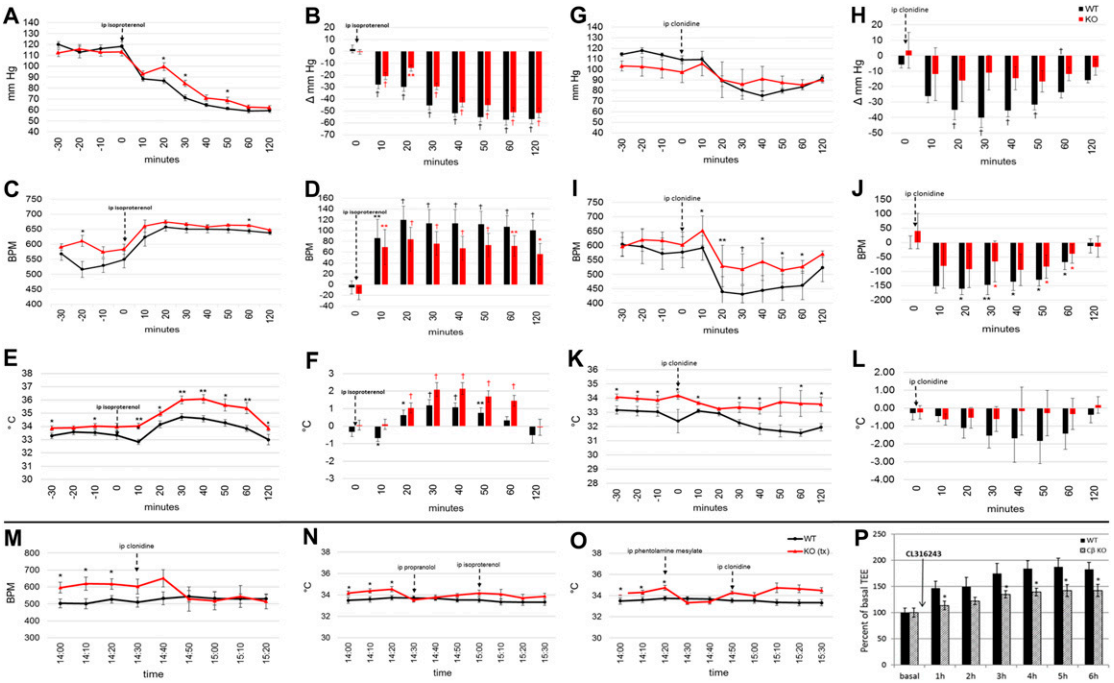

Figure 6. CβKO mice had a blunted cardiovascular response to isoproterenol and clonidine. Telemetric measurements and change from baseline for (A and B) mean BP, (C and D) HR, and (E and F) SQ temperature in response to isoproterenol (50 mg/kg) and (G and H) mean BP, (I and J) HR, and (K and L) SQ temperature in response to clonidine (40 mg/kg). Baseline values were mean values, 30 min pretreatment. Absolute values and change from baseline were compared between genotypes and within group, respectively (n = 6/group, females). (M) Clonidine corrected CβKO HR to untreated WT HR. (N) Pretreatment (tx) with propranolol (5 mg/kg) and (O) phentolamine mesylate (5 mg/kg) corrected KO SQ temperature to that of untreated WT mice (females). Mean WT values were from the same cohort and time of day. (P) Percent increase from basal TEE in HFD-fed mice after CL316243 administration. Data are means ± SEM. *$P < 0.05$; **$P < 0.01$; †$P < 0.001$ compared by multiple two-tailed Student t tests. ip, intraperitoneal.

temperature increase from baseline was significantly greater in mutant mice (Fig. 6F), making this the only mutant response that was not blunted compared with WT.

Response to clonidine was blunted in CβKO mice compared with that of WT mice. After clonidine treatment, BP decreased significantly in WT mice, from 10 minutes until 180 minutes post-treatment (Fig. 6G). In CβKO mice, the decrease in BP achieved significance only at the 60-minute time point ($P = 0.048$; Fig. 6H). The average decrease in BP for WT mice was 29 mmHg compared with 11 mmHg for mutants (Fig. 6I). The average clonidine-induced reduction in HR for the 60-minute period post-treatment was more pronounced in WT compared with CβKO mice [132 beats/minute (BPM) and 76 BPM, respectively; Fig. 6J]. Likewise, CβKO mice were resistant to the effect of clonidine in decreasing SQ temperature (Fig. 6K), as the mean SQ temperature of CβKO mice showed little to no post-treatment suppression (Fig. 6L).

Importantly, clonidine was able to correct the elevated HR of CβKO mice to the average HR of untreated WT littermates (Fig. 6M). We also found that the elevated SQ temperature of CβKO mice was transiently normalized to a level comparable to that of untreated WT mice by treatment with either propranolol or phentolamine mesylate, β- and α-adrenergic receptor antagonists, respectively (Fig. 6N and 6O). For these analyses, we compared the measurements of treated CβKO mice with those of the WT mice from the same telemetry cohort at the same time of day, which were recorded during a 24-hour basal telemetry experiment.

We also tested the metabolic response to specific β3-adrenergic receptor stimulation using CL316243 in a cohort of mice used for an indirect calorimetry experiment. HFD-fed mice, but

not CD-fed (data not shown) CβKO, displayed a blunted response to CL316243 compared with WT mice, as shown by the percent increase in TEE (Fig. 6P).

3. Discussion

High worldwide obesity rates and persisting lifestyle factors that support those rates pose a major global health threat. The increasing metabolic rate to promote weight loss by targeted pharmacologic stimulation of BAT and of WAT to initiate conversion to "beige" AT has been an active area of research in the battle against obesity (for thorough review, see Warner and Mittag [43] and Kajimura *et al.* [44]). A high concentration of mitochondria and the potent ability to oxidize lipids contrast BAT from WAT and enable nonshivering thermogenesis to maintain body temperature at subthermoneutral temperatures and increased TEE, particularly during HFD feeding. Enhanced energy expenditure and SQ temperature and locomotor activity played a role in the DIO resistance, observed in male and female CβKO mice, respectively. We hypothesized that the increased NE caused chronically elevated basal PKA activity by the increase of flux through the PKA pathway downstream of β3, in addition to the other subtypes of adrenergic receptors. This could explain the blunted response of CβKO mice to CL 316243 and other adrenergic agonists tested if the PKA system in AT and other target tissues was not responsive to further stimulation in the absence of *Prkacb* and compensatory increases in *Prkaca*. Enhanced Ucp1 protein expression in BAT (Fig. 2) lends further support to this "unthrifty" phenotype and what seemed to be a dissipation of energy as body heat in females and elevated energy expenditure in males. We replicated the previously published findings that male CβKO mice weighed less during normal chow feeding and that male and female CβKO mice gained significantly less weight during chronic HFD feeding than WT littermates (Fig. 1B) [3].

Stimulation of β3-adrenergic receptors increases energy expenditure and improves glucose tolerance [45]. Whereas energy expenditure was increased in male CβKO mice, surprisingly, it was not in female CβKO mice. The reported improvement in glucose tolerance and insulin sensitivity, which is also a characteristic of CβKO mice, may be a result of enhanced basal β3-adrenergic receptor activation, as decreased fat mass is not a robust phenotypic feature of male mutant mice despite improved glucoregulation [3].

Elevated basal NE levels support enhanced adrenergic receptor activation and are in line with elevated metabolic and HRs in CβKO mice. Clonidine, which is known to inhibit central NE release, normalized HR in CβKO mice, whereas SQ temperature was normalized by blockade of either α- or β-adrenergic receptor blockade, suggesting that enhanced catecholamine signaling was the cause of the observed increase in temperature. Additionally, the lack of increased basal PKA enzymatic activity *in vitro* or significantly increased mRNA for BAT-related genes was surprising. We saw no increase in Ucp1 in BAT at the mRNA level, but protein appeared higher, and BAT morphology clearly differed between CβKO and WT mice. It is possible that chronic activation of BAT may lead to a compensatory downregulation of *Ucp1* RNA over time in response to persistent stimulation by NE. Additionally, the assayed BAT was derived from CD-fed mice, and differences in *Ucp1* and regulation of other browning genes could emerge only under HFD-feeding conditions in parallel with the reduced adiposity that was observed only after chronic HFD exposure.

We previously showed differential regulation of the PKA system by acute and chronic HFD feeding [46]. Contrary to previous thinking, recent evidence suggests that Ucp1 can be regulated post-transcriptionally during HFD feeding in mice [47]. As thermogenesis in BAT is Ucp1 dependent [48], and we have seen that the obese *Ob/Ob* mouse had reduced thermogenic capacity, NE turnover in BAT, and decreased sympathetic activity [49], the CβKO presents an interesting phenotype with respect to thermogenic capacity. Future studies focused on the regulation of this system during HFD feeding in CβKO mice will help in better understanding how this mouse model responds to overnutrition.

Increased NE and NMN in female CβKO mice were in line with the observed increases in HR and metabolic rates and SQ temperature. In conjunction with the absence of aberrant

catecholamine production or PKA enzymatic activity in adrenal glands or other candidate tissues, these data suggest that centrally mediated, increased sympathetic outflow is likely in CβKO mice. Whereas HR was also significantly elevated in male mutants, we could not detect increased urinary catecholamines in the male CβKO mice. It seems likely that increased catecholamine secretion was too small or that interanimal variability did not permit detection of differences in male mice, despite their potential for being biologically important. The mechanism for this increased sympathetic activity remains to be determined, and the hypothesis that there is altered presympathetic-premotor neuron activity should be tested.

PKA is known to play an important and specific role in regulation of NE secretion. Activation of PKA inhibited NE exocytosis from central nervous system neurons of the LC and adrenal chromaffin cells by phosphorylation of synaptosomal nerve-associated protein 25 (SNAP-25) at Thr138, and alternatively, protein kinase C phosphorylation promoted NE exocytosis from the same cells [50]. SNAP-25 is a stabilizing component of the syntaxin, SNARE [SNAP (Soluble NSF Attachment Protein) REceptor] complex that is crucial in secretion of NE (and other neurotransmitters) via its role in vesicle membrane fusion [51]. Evidence for specificity of individual PKA subunits in brain nuclei continues to grow, and *Prkacb* is likely important in neurons that regulate the release of NE, and its deletion may not be fully compensated for by other subunits. Whereas *Prkaca* expression is higher than that of *Prkacb* in the brain (Fig. 3B), and both *Prkacb* and *Prkaca* are expressed in the LC, expression of *Prkacb* is denser throughout the LC. We chose the LC as our initial target for these studies for this reason and because *Prkacb* expression is relatively low in other key regions, such as A1/C1 cells and rostroventral lateral medulla. *Prkacb* and *Prkaca*, however, are both relatively highly expressed in nucleus tract solitarus, a region that deserves future study. Decreased PKA activity in LC, as a result of *Prkacb* deficiency, could reduce the normal inhibition of NE secretion exerted by PKA activation. Future studies will address the role of *Prkacb* in the LC and how deletion of this subunit can alter LC PKA enzymatic activity, PKA holoenzyme localization, and interactions with SNAP-25 and the SNAP REceptor (SNARE) complex.

CβKO mice reportedly resist angiotensin-II-induced cardiac hypertrophy and other cardiopathological effects [52], but no mechanism has been described. Our observations of CβKO mice confirm the absence of age-related cardiac health or other health problems. Others have linked the cardio-protective effect of PKA activation downstream of β2-adrenergic receptors to a switch of coupling from the Gs to Gi subunit of *GNAS* [53], but what may mediate such a switch is unclear. The cardioprotective effect of temperature preconditioning has implicated PKA activation and has similarly shown that consecutive PKA activation or conditioning independently could induce the same potent cardioprotection [54] and that this effect is mediated by mK_{Ca} channels [55]. Enhanced activation of PKA by chronically elevated NE may play a similar role in the CβKO mouse, which could be a useful model for studying the cardioprotective effects of conditioning of the PKA system.

The CβKO mouse is an interesting model of resistance to DIO and dysregulated glucose metabolism, as well as resistance to cardiometabolic problems. *Prkacb* disruption in mice led to increased sympathetic activation that appeared to be centrally mediated and that manifested in increased HR, SQ temperature in females, and energy expenditure in males. The observed enhancement in sympathetic outflow and downstream effects appeared to provide only beneficial health traits in the CβKO mouse and can explain DIO resistance. Further study of regulation of PKA signaling and AT activation in response to overnutrition will be valuable, as will the investigation of the mechanism by which *Prkacb* could regulate central synthesis and release of NE.

Acknowledgments

We thank Dr. Steve Soldin and Kathy Spade from the Department of Laboratory Medicine, NIH, for their help in quantifying osmolality and creatinine levels in mouse urine samples and Mirko Peitzsch and Katrin Kirsche at the Techniche Universität Dresden for processing the mouse urine samples that

were analyzed for catecholamines. We also thank G. Stanley McKnight at the Department of Pharmacology, University of Washington, for sharing his antibody against PKA Cβ.

Financial Support: This work was supported by the Eunice Kennedy Shriver National Institute of Child Health and Human Development, National Institutes of Health, Intramural Research Program (Project Z01-HD008920-01 to C.A.S.).

Correspondence: Edra London, PhD, Eunice Kennedy Shriver National Institute of Child Health and Human Development, National Institutes of Health, MSC 2425, 10 Center Drive, Bethesda, Maryland 20892. E-mail: edra.london@nih.gov.

Disclosure Summary: The authors have nothing to disclose.

References and Notes

1. Cummings DE, Brandon EP, Planas JV, Motamed K, Idzerda RL, McKnight GS. Genetically lean mice result from targeted disruption of the RII beta subunit of protein kinase A. *Nature*. 1996;**382**(6592): 622–626.
2. London E, Nesterova M, Sinaii N, Szarek E, Chanturiya T, Mastroyannis SA, Gavrilova O, Stratakis CA. Differentially regulated protein kinase A (PKA) activity in adipose tissue and liver is associated with resistance to diet-induced obesity and glucose intolerance in mice that lack PKA regulatory subunit type IIα. *Endocrinology*. 2014;**155**(9):3397–3408.
3. Enns LC, Morton JF, Mangalindan RS, McKnight GS, Schwartz MW, Kaeberlein MR, Kennedy BK, Rabinovitch PS, Ladiges WC. Attenuation of age-related metabolic dysfunction in mice with a targeted disruption of the Cbeta subunit of protein kinase A. *J Gerontol A Biol Sci Med Sci*. 2009;**64**(12): 1221–1231.
4. Planas JV, Cummings DE, Idzerda RL, McKnight GS. Mutation of the RIIbeta subunit of protein kinase A differentially affects lipolysis but not gene induction in white adipose tissue. *J Biol Chem*. 1999; **274**(51):36281–36287.
5. Schreyer SA, Cummings DE, McKnight GS, LeBoeuf RC. Mutation of the RIIbeta subunit of protein kinase A prevents diet-induced insulin resistance and dyslipidemia in mice. *Diabetes*. 2001;**50**(11): 2555–2562.
6. Yang L, McKnight GS. Hypothalamic PKA regulates leptin sensitivity and adiposity. *Nat Commun*. 2015;**6**(1):8237.
7. Enns LC, Morton JF, Treuting PR, Emond MJ, Wolf NS, Dai DF, McKnight GS, Rabinovitch PS, Ladiges WC. Disruption of protein kinase A in mice enhances healthy aging. *PLoS ONE*. 2009;**4**(6): e5963.
8. Nolan MA, Sikorski MA, McKnight GS. The role of uncoupling protein 1 in the metabolism and adiposity of RII beta-protein kinase A-deficient mice. *Mol Endocrinol*. 2004;**18**(9):2302–2311.
9. Guthrie CR, Skâlhegg BS, McKnight GS. Two novel brain-specific splice variants of the murine Cbeta gene of cAMP-dependent protein kinase. *J Biol Chem*. 1997;**272**(47):29560–29565.
10. Desseyn JL, Burton KA, McKnight GS. Expression of a nonmyristylated variant of the catalytic subunit of protein kinase A during male germ-cell development. *Proc Natl Acad Sci USA*. 2000;**97**(12): 6433–6438.
11. Brandon EP, Idzerda RL, McKnight GS. PKA isoforms, neural pathways, and behaviour: making the connection. *Curr Opin Neurobiol*. 1997;**7**(3):397–403.
12. Howe DG, Wiley JC, McKnight GS. Molecular and behavioral effects of a null mutation in all PKA C beta isoforms. *Mol Cell Neurosci*. 2002;**20**(3):515–524.
13. Stratakis CA. Cushing syndrome caused by adrenocortical tumors and hyperplasias (corticotropin-independent Cushing syndrome). *Endocr Dev*. 2008;**13**:117–132.
14. Cypess AM, Lehman S, Williams G, Tal I, Rodman D, Goldfine AB, Kuo FC, Palmer EL, Tseng YH, Doria A, Kolodny GM, Kahn CR. Identification and importance of brown adipose tissue in adult humans. *N Engl J Med*. 2009;**360**(15):1509–1517.
15. van Marken Lichtenbelt WD, Vanhommerig JW, Smulders NM, Drossaerts JM, Kemerink GJ, Bouvy ND, Schrauwen P, Teule GJ. Cold-activated brown adipose tissue in healthy men. *N Engl J Med*. 2009; **360**(15):1500–1508.
16. Cypess AM, Weiner LS, Roberts-Toler C, Franquet Elía E, Kessler SH, Kahn PA, English J, Chatman K, Trauger SA, Doria A, Kolodny GM. Activation of human brown adipose tissue by a β3-adrenergic receptor agonist. *Cell Metab*. 2015;**21**(1):33–38.
17. Dickson LM, Gandhi S, Layden BT, Cohen RN, Wicksteed B. Protein kinase A induces UCP1 expression in specific adipose depots to increase energy expenditure and improve metabolic health. *Am J Physiol Regul Integr Comp Physiol*. 2016;**311**(1):R79–R88.

18. London E, Rothenbuhler A, Lodish M, Gourgari E, Keil M, Lyssikatos C, de la Luz Sierra M, Patronas N, Nesterova M, Stratakis CA. Differences in adiposity in Cushing syndrome caused by PRKAR1A mutations: clues for the role of cyclic AMP signaling in obesity and diagnostic implications. *J Clin Endocrinol Metab*. 2014;**99**(2):E303–E310.
19. Lateef DM, Xiao C, Brychta RJ, Diedrich A, Schnermann J, Reitman ML. Bombesin-like receptor 3 regulates blood pressure and heart rate via a central sympathetic mechanism. *Am J Physiol Heart Circ Physiol*. 2016;**310**(7):H891–H898.
20. Wallner M, Duran JM, Mohsin S, Troupes CD, Vanhoutte D, Borghetti G, Vagnozzi RJ, Gross P, Yu D, Trappanese DM, Kubo H, Toib A, Sharp TE III, Harper SC, Volkert MA, Starosta T, Feldsott EA, Berretta RM, Wang T, Barbe MF, Molkentin JD, Houser SR. Acute catecholamine exposure causes reversible myocyte injury without cardiac regeneration. *Circ Res*. 2016;**119**(7):865–879.
21. Nonogaki K, Kaji T. α1-Adrenergic receptor downregulates hepatic FGF21 production and circulating FGF21 levels in mice. *Neurosci Lett*. 2017;**638**:35–38.
22. RRID:AB_2268772, https://scicrunch.org/resolver/AB_2268772.
23. RRID:AB_397944, https://scicrunch.org/resolver/AB_397944.
24. RRID:AB_2304265, https://scicrunch.org/resolver/AB_2304265.
25. RRID:AB_2340390, https://scicrunch.org/resolver/AB_2340390.
26. RRID:AB_10015282, https://scicrunch.org/resolver/AB_10015282.
27. RRID:AB_2340770, https://scicrunch.org/resolver/AB_2340770.
28. RRID:AB_572268, https://scicrunch.org/resolver/AB_572268.
29. RRID:AB_2336528, https://scicrunch.org/resolver/AB_2336528.
30. RRID:AB_2561044, https://scicrunch.org/resolver/AB_2561044.
31. RRID:AB_162543, https://scicrunch.org/resolver/AB_162543.
32. RRID:AB_2535853, https://scicrunch.org/resolver/AB_2535853.
33. RRID:AB_2783820, https://scicrunch.org/resolver/AB_27823820.
34. RRID:AB_2536183, https://scicrunch.org/resolver/AB_2536183.
35. Nesterova M, Yokozaki H, McDuffie E, Cho-Chung YS. Overexpression of RII beta regulatory subunit of protein kinase A in human colon carcinoma cell induces growth arrest and phenotypic changes that are abolished by site-directed mutation of RII beta. *Eur J Biochem*. 1996;**235**(3):486–494.
36. Peitzsch M, Pelzel D, Glöckner S, Prejbisz A, Fassnacht M, Beuschlein F, Januszewicz A, Siegert G, Eisenhofer G. Simultaneous liquid chromatography tandem mass spectrometric determination of urinary free metanephrines and catecholamines, with comparisons of free and deconjugated metabolites. *Clin Chim Acta*. 2013;**418**:50–58.
37. Cadd G, McKnight GS. Distinct patterns of cAMP-dependent protein kinase gene expression in mouse brain. *Neuron*. 1989;**3**(1):71–79.
38. Amieux PS, McKnight GS. The essential role of RI alpha in the maintenance of regulated PKA activity. *Ann N Y Acad Sci*. 2002;**968**(1):75–95.
39. Greene EL, Horvath AD, Nesterova M, Giatzakis C, Bossis I, Stratakis CA. In vitro functional studies of naturally occurring pathogenic PRKAR1A mutations that are not subject to nonsense mRNA decay. *Hum Mutat*. 2008;**29**(5):633–639.
40. Newell-Price J, Bertagna X, Grossman AB, Nieman LK. Cushing's syndrome. *Lancet*. 2006;**367**(9522):1605–1617.
41. Eisenhofer G, Huynh TT, Hiroi M, Pacak K. Understanding catecholamine metabolism as a guide to the biochemical diagnosis of pheochromocytoma. *Rev Endocr Metab Disord*. 2001;**2**(3):297–311.
42. Nam H, Kerman IA. Distribution of catecholaminergic presympathetic-premotor neurons in the rat lower brainstem. *Neuroscience*. 2016;**324**:430–445.
43. Warner A, Mittag J. Breaking BAT: can browning create a better white? *J Endocrinol*. 2016;**228**(1):R19–R29.
44. Kajimura S, Spiegelman BM, Seale P. Brown and beige fat: physiological roles beyond heat generation. *Cell Metab*. 2015;**22**(4):546–559.
45. Xiao C, Goldgof M, Gavrilova O, Reitman ML. Anti-obesity and metabolic efficacy of the β3-adrenergic agonist, CL316243, in mice at thermoneutrality compared to 22°C. *Obesity (Silver Spring)*. 2015;**23**(7):1450–1459.
46. London E, Nesterova M, Stratakis CA. Acute vs chronic exposure to high fat diet leads to distinct regulation of PKA. *J Mol Endocrinol*. 2017;**59**(1):1–12.
47. Takahashi A, Adachi S, Morita M, Tokumasu M, Natsume T, Suzuki T, Yamamoto T. Post-transcriptional stabilization of Ucp1 mRNA protects mice from diet-induced obesity. *Cell Reports*. 2015;**13**(12):2756–2767.

48. Golozoubova V, Hohtola E, Matthias A, Jacobsson A, Cannon B, Nedergaard J. Only UCP1 can mediate adaptive nonshivering thermogenesis in the cold. *FASEB J*. 2001;**15**(11):2048–2050.
49. Knehans AW, Romsos DR. Reduced norepinephrine turnover in brown adipose tissue of ob/ob mice. *Am J Physiol*. 1982;**242**(4):E253–E261.
50. Gao J, Hirata M, Mizokami A, Zhao J, Takahashi I, Takeuchi H, Hirata M. Differential role of SNAP-25 phosphorylation by protein kinases A and C in the regulation of SNARE complex formation and exocytosis in PC12 cells. *Cell Signal*. 2016;**28**(5):425–437.
51. Duman JG, Forte JG. What is the role of SNARE proteins in membrane fusion? *Am J Physiol Cell Physiol*. 2003;**285**(2):C237–C249.
52. Enns LC, Bible KL, Emond MJ, Ladiges WC. Mice lacking the Cβ subunit of PKA are resistant to angiotensin II-induced cardiac hypertrophy and dysfunction. *BMC Res Notes*. 2010;**3**(1):307.
53. Tong H, Bernstein D, Murphy E, Steenbergen C. The role of beta-adrenergic receptor signaling in cardioprotection. *FASEB J*. 2005;**19**(8):983–985.
54. Khaliulin I, Parker JE, Halestrap AP. Consecutive pharmacological activation of PKA and PKC mimics the potent cardioprotection of temperature preconditioning. *Cardiovasc Res*. 2010;**88**(2):324–333.
55. Heinen A, Ströthoff M, Schmidt A, Stracke N, Behmenburg F, Bauer I, Hollmann MW, Huhn R. Pharmacological options to protect the aged heart from ischemia and reperfusion injury by targeting the PKA-BK(Ca) signaling pathway. *Exp Gerontol*. 2014;**56**:99–105.